Research Article
Open Access
CrossMark

Homotopy analysis method to MHD-slip flow of an upper- convected maxwell viscoelastic nanofluid in a permeable channel embedded in a porous medium

Abstract

The expanding applications of viscoelastic fluids in biomedical engineering and industrial processes require proper under and physical insights into the flow phenomena of the fluids. In this work, simultaneous effects of slip and magnetic field on the flow of an upper convected Maxwell (UCM) nano fluid through a permeable micro channel embedded in porous medium are analyzed using homotopy analysis method. The results of the approximate analytical solution depict very good agreements with the results of the fifth-order Runge-Kutta Fehlberg method (Cash-Karp Runge-Kutta) coupled with shooting methodfor the verification of the mathematical method used in analyzing the flow. Thereafter, the obtained analytical solutions are used to investigate the effects of pertinent rheological parameters on flow. It is observed from the results that increase in slip parameter, nano particle concentration and Darcy number lead to increase in the velocity of the upper-convected Maxwell fluid while increase in Deborah's, Hartmann, and Reynold numbers decrease the fluid flow velocity towards the lower plate but as the upper plate is approached a reverse trend is observed. The study can be used to advance the application of upper convected Maxwell flow in the areas of in biomedical, geophysical and astrophysics.

Keywords: slip analysis, upper-convected maxwell flow, viscoelastic nano fluid, magnetic field, porous medium

Volume 5 Issue 1 - 2020

MG Sobamowo, A A Yinusa, AT Akinshilo, ST Aladenusi
Department of Mechanical Engineering, University of Lagos, Akoka, Lagos, Nigeria

Correspondence: M G Sobamowo, Department of Mechanical Engineering, University of Lagos, Akoka, Lagos, Nigeria, Email mikegbeminiy@gmail.com

Received: January 01, 2020 | **Published:** March 18, 2020

Introduction

The vast areas of applications and the importance of the viscoelastic fluid flow in modern science and engineering such as gaseous diffusion, blood flow through oxygenators, flow in blood capillaries have continue to aroused the research interests. Complex rheological fluids such as blood, paints, synovial fluid, saliva, jam which cannot be adequately described by Navier Stokes. This lead to the development of complex constitutive relations to capture the flow behaviour of the complex fluids.[1] Among the newly developed fluid models of the integral and differential-type models, Upper convected Maxwell fluid model has showed to be an effective fluid model that capture these phenomena of fluids especially of those with high elastic behaviours such as polymer melts. Since highly elastic fluids have high Deborah number.[2,3] In the analysis of Maxwell flow, Fetecau[4] presented a new exact solution for flow though infinite micro channel while Hunt[5] studied convective fluid flow through rectangular duct. Sheikholeslami et al.[6] investigated magneto hydrodynamic field effect on flow through semi-porous channel utilizing analytical methods. Shortly after, Sheikholeslami[7-9] adopted numerical solutions in the investigations of nanofluid in semi-annulus enclosure. Flow of upper convected Maxwell fluid through porous stretch sheet was investigated by Raftari and Yildirim.[10] Entophy generation in fluid in the presence of magnetic field was analyzed by Sheikholeslami and Ganji [11] using lattice Boltzman method while Ganji et al.[12] used analytical and numerical methods for the fluid flow problems under the influence of magnetic field. The flow of Viscoelastic fluid through a moving plate was analyzed by Sadeghy and Sharifi [13] using local similarity solutions. Mass transfer and flow of chemically reactive upper convected Maxwell fluid under induced magnetic field was investigated by Vajrevulu et al.[14] Not long after Raftari and Vajrevulu[15] adopted the homotopy analysis method in the study of flow and heat transfer in stretching wall channels considering MHD. Hatamiet al.[16] presented forced convective MHD nano fluid flow conveyed through horizontal parallel plates. Laminar thermal boundary flow layer over flat plate considering convective fluid surface was analyzed by Aziz [17] using similarity solution. Beg and Makinde[18] examined the flow of viscoelastic fluid through Darcian microchannel with high permeability.

Most of the above reviews studies focused on the analysis of fluid flow under no slip condition. However, such an assumption of no slip condition does not hold in a flow system with small size characteristics size or low flow pressure. The pioneer work of flow with slip boundary condition was first initiated by Navier.[19] Such an important condition (slip conditions) occur in various flows such as nano fluids, polymeric liquids, fluids containing concentrated suspensions, flow on multiple interfaces, thin film problems and rarefied fluid problems.[19–31] Due to the practical implications of the condition of flow processes, several studies on the effects of slip boundary conditions on fluids flow behaviours have been presented by many researchers.[19–32] Abbasi et al.[33] investigated the MHD flow characteristics of upper-convicted Maxwell viscoelastic flow in a permeable channel under slip conditions. However, an analytical study on simultaneous effects of slip, magnetic field, nano particle and porous medium on the flow characteristics of an upper-convected Maxwell viscoelastic nano fluid has not been carried out in literature. Therefore, in this work, slip flow analysis of an upper-convected Maxwell viscoelastic nano fluid through a permeable micro channel embedded in porous medium under the influence of magnetic field is analyzed. The nonlinear partial differential equations governing the flow phenomena are converted to a nonlinear ordinary differential

equation using similarity transformation. Thereafter, the ordinary differential is solved using homotopy analysis method.

Model Development and Analytical Solution

Consider a laminar slip flow of an electrically conducting fluid in a microchannel is considered. Along the y axis, magnetic field are imposed uniformly, as described in the physical model diagram (Figure 1) It is assumed external electric field is zero and constant of electrical conductivity is constant. Therefore, magnetic Reynolds number is smalland magnetic field induced by fluid motion is negligible.

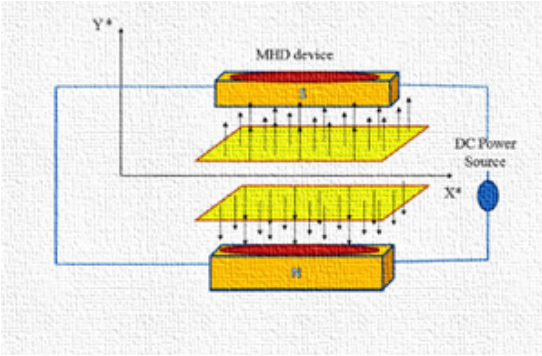

Figure 1 Flow of upper-convected Maxwell fluid between in permeable channel embedded in porous medium.

Based on the assumptions, the governing equation for the Maxwell fluid is presented as [8]

$$T - pI + S \tag{1}$$

Where the Cauchy stress tensor is T and S is the extra-stress Tensor which satisfies

$$S + \lambda\left(\frac{ds}{dt} - LS - SL^T\right)\mu A_L \tag{2}$$

The Rivlin-Ericksen tensor is defined by

$$A_L = \nabla V + \left(\nabla V\right)^T \tag{3}$$

The continuity and momentum equation's for steady, incompressible two dimensional flows are expressed as

$$\frac{\partial \overline{u}}{\partial x} + \frac{\partial \overline{v}}{\partial y} = 0 \tag{4}$$

$$\rho_{nf}\left(u\frac{\partial u}{\partial x} + v\frac{\partial u}{\partial y}\right) = -\frac{\partial P}{\partial x} + \frac{\partial S_{xx}}{\partial x} + \frac{\partial S_{xy}}{\partial y} - \sigma_{nf}B^2(t)u - \frac{\mu_{nf}u}{K_p}, \tag{5}$$

$$\rho_{nf}\left(\overline{u}\frac{\partial \overline{v}}{\partial x} + \overline{v}\frac{\partial \overline{v}}{\partial y}\right) = -\frac{\partial P}{\partial x} + \frac{\partial S_{yx}}{\partial x} + \frac{\partial S_{yy}}{\partial y} - \frac{\mu_{nf}\overline{v}}{K_p}, \tag{6}$$

wherethe effective density *pnf* and effective dynamic viscosity μ_{nf} of the nanofluid are defined as follows:

$$\rho_{nf} = \left(1-\phi\right)\rho_f + \phi\rho_s, \tag{7}$$

$$\mu_{nf} = \frac{\mu_f}{\left(1-\phi\right)^{2.5}}, \tag{8}$$

$$\sigma_{nf} = \sigma_f\left[1 + \frac{3\left\{\frac{\sigma_s}{\sigma_f} - 1\right\}\phi}{\left\{\frac{\sigma_s}{\sigma_f} + 2\right\}\phi - \left\{\frac{\sigma_s}{\sigma_f} - 1\right\}\phi}\right], \tag{9}$$

S_{xx},S_{xy},S_{yx} and S_{yy} are extra stress tensors and ρ is the density of the fluid.

Using the shear-stress strain for a upper-convected liquid, The governing equations of fluid motion is easily expressed as

$$\frac{\partial u}{\partial x} + \frac{\partial v}{\partial y} = 0 \tag{10}$$

$$u\frac{\partial u}{\partial x} + v\frac{\partial u}{\partial y} + \lambda\left(u^2\frac{\partial^2 u}{\partial x^2} + v\frac{\partial^2 u}{\partial y^2} + 2uv\frac{\partial^2 u}{\partial x\partial y}\right) = v_{nf}\frac{\partial^2 u}{\partial y^2} - \frac{\sigma_{nf}B^2(t)u}{\rho_{nf}} - \frac{v_{nf}u}{K_p}, \tag{11}$$

where flow velocity component (u,v) are velocity component along the xand y directions respectively. Since flow is symmetric about channel center line, attention is given to the flow region $0<y<H$. Appropriate boundary condition is given as [14]:

$$y = 0 : \frac{\partial u}{\partial x} = 0, v = 0 \tag{12}$$

$$y = H : \frac{\partial u}{\partial y} = -\beta u, \quad v = V_w \tag{13}$$

where $V_w$and β are the wall characteristic suction velocity and sliding friction respectively.

The physical and thermal properties of the base fluid and nano particles are given in Table 1 and Table 2, respectively.

The similarity variables are introduced as:

$$\eta = \frac{y}{H}, \quad u = -V_w x f'(y); \quad v = V_w f(y); \quad k = \frac{\mu}{H\beta} \tag{14}$$

With the aid of the dimensionless parameters in Eq. (14), the constitutive relation is satisfied. Equation (2-4) can be expressed as:

$$f''' - \left(M^2 + \frac{1}{Da}\right)f' + \left(1-\phi\right)^{2.5}\left(\left(1-\phi\right) + \phi\frac{\rho_s}{\rho_f}\right)Re_w\left(f'^2 - ff''\right) + De\left(1-\phi\right)^{2.5}\left(2ff'f'' - f^2f'''\right) = 0 \tag{15}$$

And the boundary conditions as

$$\begin{aligned} &\eta = 0 : f'' = 0; f = 0 \\ &\eta = 1 : f' = -kf'' : f = 1 \end{aligned} \tag{16}$$

where $\mathrm{Re}_w = \frac{V_w H}{\upsilon}$ is the Reynolds number, $De = \frac{\lambda V_w^2}{\upsilon}$ is the Deborah's number, $M^2 = \frac{\sigma B_0^2 H}{\mu}$ is the Hartman parameter, $Da = \frac{K_p}{H}$ is the Darcy's number. For Re_w>0 corresponds to suction flow while Re_w<0 correspond to injection flow respectively.

Equ. (13) is a third-order differential equation with four boundary conditions. Through a creative differentiation of Eq. (12). Hence introducing fourth order equation as:

$$f^{iv}-\left(M^2+\frac{1}{Da}\right)f''+(1-\phi)^{2.5}\left((1-\phi)+\phi\frac{\rho_s}{\rho_f}\right)Re_w\left(ff''-ff'''\right)+De(1-\phi)^{2.5}\left(2f'^2f''-2ff''^2+f^2f^{iv}\right)=0 \tag{17}$$

The above Eq. (17) study satisfies all the four boundary conditions

Table 1 Physical and thermal properties of the base fluid

Base fluid	ρ (kg/m3)	Cp (J/kgK)	k (W/mK)	σ(Ω-1m-1)
Pure water	997.1	4179	0.613	5.50
Ethylene Glycol	1115	2430	0.253	1.07
Engine oil	884	1910	0.144	4.02
Kerosene	783	2010	0.145	4.01

Table 2 Physical and thermal properties of nanoparticles

Nanoparticles	ρ (kg/m3)	Cp (J/kgK)	k (W/mK)	σ(Ω-1m-1)
Copper (Cu)	8933	385	401	59.6
Aluminum oxide (Al2O3)	3970	765	40	16.7
SWCNTs	2600	42.5	6600	1.26
Silver (Ag)	10500	235.0	429	
Titanium dioxide (TiO2)	4250	686.2	8.9538	
Copper (II) Oxide (CuO)	783	540	18	

Application of the Homotopy Analysis Method to the Flow Problem

The homotopy analysis method (HAM) which is an analytical scheme for providing approximate solutions to the ordinary differential equations, is adopted in generating solutions to the ordinary nonlinear differential equations .Upon constructing the homotopy, the initial guess and auxiliary linear operator can be expressed as

$$f_0(\eta)=-\frac{1}{2(3k+1)}\eta^3+\frac{3(2k+1)}{2(3k+1)}\eta \tag{18}$$

$$L(f)=f'''' \tag{19}$$

$$L\left(\frac{1}{6}c_1\eta^3+\frac{1}{2}c_2\eta^2+c_3\eta+c_4\right)=0 \tag{20}$$

Where $C_i\left(i=1,2,3,4\right)$ are constants? Let $P=\in[0,1]$ connotes the embedding parameter and $\hbar$ is the non-zero auxiliary parameter. Therefore, the homogony is constructed as

Zeroth-order deformation equations

$$(1-P)L\left[F(\eta;p)-f_0(\eta)\right]=p\hbar H(\eta)N\left[F(\eta;p)\right] \tag{21}$$

$$F(0;p)=0;\ F'(0;p)=0\ ;F(1;\mathrm{p})=1\ ;kF'(1;\mathrm{p})+F'(1;p)=0 \tag{22}$$

$$N[F(\eta;p)]=\frac{d^4F(\eta;p)}{d\eta^4}+(1-\phi)^{2.5}\left((1-\phi)+\phi\frac{\rho_s}{\rho_f}\right)Re_w\left[\frac{dF(\eta;\mathrm{p})}{d\eta}\frac{d^2F(\eta;p)}{d\eta^2}-F(\eta;p)\frac{d^3(\eta;p)}{d\eta^3}\right]$$
$$-M^2\frac{d^2F(\eta;p)}{d\eta^2}-\frac{1}{Da}\frac{d^2F(\eta;p)}{d\eta^2}+De(1-\phi)^{2.5}\left[\begin{array}{l}2\left(\frac{dF(\eta;\mathrm{p})}{d\eta}\right)^2\frac{d^2F(\eta;p)}{d\eta^2}-2F(\eta;\mathrm{p})\left(\frac{d^2F(\eta;p)}{d\eta^2}\right)^2\\+(f(\mathrm{y};\mathrm{p}))^2\frac{d^4F(\eta;p)}{d\eta^4}\end{array}\right] \tag{23}$$

when $p=0$ and $p=1$ we have

$$F(\eta;0)=f_0(\eta)\ ;F(\eta;1)=f(\eta) \tag{24}$$

As p increases from *0 to 1*. $F_{(y;p)}$ varies from $f_0(y)$ to $f(y)$. By Taylor's theorem and utilizing Eq. (26),*F(y; p)* can be expanded in the power series of p as follows:

$$F(\eta;p)=f_0(\eta)+\sum_{m-1}^{\infty}f_m(\eta)p^m, f_m(\eta)=\frac{1}{m!}\left.\frac{\partial^m(F(\eta;p))}{\partial p^m}\right|_{p=0} \tag{25}$$

Citation: Sobamowo MG, Yinusa AA, Akinshilo AT, et al. Homotopy analysis method to MHD-slip flow of an upper- convected maxwell viscoelastic nanofluid in a permeable channel embedded in a porous medium. *Int J Petrochem Sci Eng.* 2020;5(1):11–20. DOI: 10.15406/ipcse.2020.05.00118

where $\hbar$ is chosen such that the series is convergent at p = 1; therefore, by Eq. (24) it is easily shown that

$$f(\eta) = f_0(\eta) + \sum_{m-1}^{\infty} f_m(\eta) \tag{26}$$

mth order deformation equations

$$L[f_m(\eta) - \chi_m f_{m-1}(\eta)] = \hbar H(\eta) R_m(\eta) \tag{27}$$

$$F_m(0;p) = 0;\ F^{"}(0;p) = 0\ ;\ F_m(1,p) = 0\ ;\ kF_m^{"}(1;p) + F_m^{'}(1,p) = 0 \tag{28}$$

$$\begin{aligned} R_m(\eta) = f_{m-1}^{""} + \sum_{k=0}^{m-1} \Bigg[& (1-\phi)^{2.5}\left((1-\phi) + \phi\frac{\rho_s}{\rho_f}\right) Re_w\left(f_{m-1}^{'} f_k^{"} - f_{m-1-k} f_k^{'''}\right) + De(1-\phi)^{2.5} f_{m-1-k}^{'}\left(\sum_{l=0}^{k}\left(2 f_{k-l}^{'} f_l^{"}\right)\right) \\ & -De(1-\phi)^{2.5} f_{m-1-k}\left(\sum_{l=0}^{k}\left(2 f_k^{"} -_l f^{"} - f_{k-l} f_l^{'''}\right)\right) \Bigg] \\ & - M^2 f_{m-1}^{"} - \frac{1}{Da} f_{m-1}^{"} \end{aligned} \tag{29}$$

Now the results for the convergence, differential equation and the auxiliary function are determined according to the solution expression. So we assume

$$H(y) = 1 \tag{30}$$

The analytic solution is deve,loped using the MATLAB computational stencil. Hence the first deformation is expressed below

$$\begin{aligned} f_1(\eta) = \hbar \Bigg\{ & -\frac{5}{672}\frac{De(1-\phi)^{2.5}\eta^9}{(3k+1)} - \frac{3}{2}\frac{\left(\begin{array}{l} -0.0071649(1-\phi)^{2.5}\left((1-\phi)+\phi\frac{\rho_s}{\rho_f}\right)Re_w - 0.042857De - \\ 0.0023810(1-\phi)^{2.5}\left((1-\phi)+\phi\frac{\rho_s}{\rho_f}\right)Re_w - 0.085714Dek \end{array}\right)\eta^7}{27k^3+27k^2+9k+1} \\ & -\frac{3}{2}\frac{\left(\begin{array}{l} -0.15\left(M^2+\frac{1}{Da}\right)k^2 - 0.1\left(M^2+\frac{1}{Da}\right)k - 0.016667\left(M^2+\frac{1}{Da}\right) + 0.3Dek^2 \\ +0.3De(1-\phi)^{2.5}k + 0.075De(1-\phi)^{2.5} \end{array}\right)\eta^5}{27k^3+27k^2+9k+1} \\ & +\frac{1}{840}\Bigg[\frac{\left(\begin{array}{l} 378De(1-\phi)^{2.5}k^3 - 1890\left(M^2+\frac{1}{Da}\right)k^3 - 189(1-\phi)^{2.5}\left((1-\phi)+\phi\frac{\rho_s}{\rho_f}\right)Re_w k^2 + 2268DDe(1-\phi)^{2.52} - \\ 1638\left(M^2+\frac{1}{Da}\right)k^2 - 90(1-\phi)^{2.5}\left((1-\phi)+\phi\frac{\rho_s}{\rho_f}\right)Re_w k - 462\left(M^2+\frac{1}{Da}\right)k + 468De(1-\phi)^{2.5}k \end{array}\right)\eta^3}{1+54k^2+12k+108k^3+81k^4} \\ & +\frac{\left(-9(1-\phi)^{2.5}\left((1-\phi)+\phi\frac{\rho_s}{\rho_f}\right)Re_w + 52De(1-\phi)^{2.5} - 42\left(M^2+\frac{1}{Da}\right)\right)}{1+54k^2+12k+108k^3+81k^4}\Bigg] \\ & -\frac{1}{1120}\Bigg[\frac{\left(\begin{array}{l} -8(1-\phi)^{2.5}\left((1-\phi)+\phi\frac{\rho_s}{\rho_f}\right)Re_w - 96(1-\phi)^{2.5}\left((1-\phi)+\phi\frac{\rho_s}{\rho_f}\right)Re_w k - 1764\left(M^2+\frac{1}{Da}\right)k^3 \\ +1440De(1-\phi)^{2.5}k^2 + 77De(1-\phi)^{2.5}k - 364\left(M^2+\frac{1}{Da}\right)k \end{array}\right)\eta}{1+54k^2+12k+108k^3+81k^4} + \\ & \frac{\left(\begin{array}{l} -1428\left(M^2+\frac{1}{Da}\right)k^2 + 3528De(1-\phi)^{2.5}k^3 - 216(1-\phi)^{2.5}\left((1-\phi)+\phi\frac{\rho_s}{\rho_f}\right)Re_w k^2 \\ -28\left(M^2+\frac{1}{Da}\right) + 7De(1-\phi)^{2.5} \end{array}\right)\eta}{1+54k^2+12k+108k^3+81k^4}\Bigg] \Bigg\} \end{aligned} \tag{31}$$

Similarly, $f_2(\eta), f_3(\eta), f_4(\eta), f_5(\eta)\ldots$ are found but they are too large expressions that cannot be included in this paper. However, they are included in the results displayed graphically.

Convergence of the HAM solution

It is established that the convergence and the rate of approximation for the HAM solution strongly depend on the value of the auxiliary parameter. [34–37]The present problem shows a wide of acceptable range of values of $\hbar$ for the difference controlling parameters of the model as shown in (Tables 3a-3d.).

Table 3a The results of admissible range of values for $\hbar$ whenRew=-7.5 De= 0.12, ϕ=0.08

M	DA	K=0.1 K=0.9
0.5	2.0-2.0 < 0.2	-1.4< <0.4
1.0	1.0-1.4< $\hbar$ <0.3	-1.1< $\hbar$ <0.0
2.0	1.0-1.1< 0.5	-0.8 < $\hbar$ <0.0
2.0	0.5-0.8 < $\hbar$ <0.0	-0.6< $\hbar$ <0.0
3.0	0.5-0.6< $\hbar$ <0.0	-0.5< $\hbar$ <0.0

Table 3b The results of admissible range of values for $\hbar$ whenRew=7.5 De= 1.10, ϕ=0.08

M	Da	k =0.1	k=0.9
0.5	2.0	-0.8< $\hbar$ <-0.4	-0.7< $\hbar$ <-0.4
1.0	1.0	-0.7< $\hbar$ <0.4	-0.8< $\hbar$ <-0.4
2.0	1.0	-0.1< $\hbar$ <0.0	-1.0< $\hbar$ <-0.1
2.0	0.5	-1.2< $\hbar$ <0.1	-1.0< $\hbar$ <0.0

Table 3c The results of admissible range of values for $\hbar$ whenRew=-7.5 De= 1.10, ϕ=0.08

M	Da	k =0.1	k=0.9
0.5	2.0	1.5< $\hbar$ <0.1	-1.8< $\hbar$ <0.0
1.0	1.0	1.7< $\hbar$ <0.1	-1.4< $\hbar$ <0.1
2.0	0.5	-0.7< $\hbar$ <0.1	-0.7< $\hbar$ <0.0
2.0	0.5	-0.6 < $\hbar$ <0.0	-0.5< $\hbar$ <0.0
3.0	0.5	-0.6< $\hbar$ <0.0	-0.5< $\hbar$ <0.0

Table 3d The results of admissible range of values for $\hbar$ whenRew=7.5 De= 1.10, ϕ=0.08

M	Da	k =0.1	k=0.9
0.5	2.0	-1.8< $\hbar$ <-0.5	-19< $\hbar$ <0.0
1.0	1.0	-2.2< $\hbar$ <-0.5	-2.0< $\hbar$ <0.0
2.0	0.5	-0.7< $\hbar$ <0.0	-1.5< $\hbar$ <0.0
3.0	0.5	-1.0< $\hbar$ <0.0	-1.4< $\hbar$ <0.1

Numerical Procedure for the analysis of the governing equation

Eq. (15) is a fourth-order ordinary differential equation which is in this work is analyzed numerically using fifth-order Runge-Kutta Fehlberg method (Cash-Karp Runge-Kutta) coupled with shooting method. Since Runge-Kutta method is for solving first-order ordinary differential equation, the fourth-order ordinary differential equation is decomposed into a system of first-order differential equations as follows:

$$f' = p, \tag{32}$$

$$f'' = p' = q, \tag{33}$$

$$f''' = q' = w,$$

$$f^{iv} = w' = z, \tag{34}$$

$$z = \left(M^2 + \frac{1}{Da}\right)p - (1-\phi)^{2.5}\left((1-\phi) + \phi\frac{\rho_s}{\rho_f}\right)Re_w\left(p^2 - fq\right) - De(1-\phi)^{2.5}\left(2fpq - f^2w\right)$$

The above Eqs. (29)-(31) can be written as

$$a(\eta, f, p, q, w, z) = p, \tag{35}$$

$$b(\eta, f, p, q, w, z) = q, \tag{36}$$

$$c(\eta, f, p, q, w, z) = w, \tag{37}$$

$$d(\eta, f, p, q, w, z) = z \tag{38}$$

$$e(\eta, f, p, q, z) = \left(M^2 + \frac{1}{Da}\right)p - (1-\phi)^{2.5}\left((1-\phi) + \phi\frac{\rho_s}{\rho_f}\right)Re_w\left(p^2 - fq\right) - De(1-\phi)^{2.5}\left(2fpq - f^2w\right) \tag{39}$$

The iterative scheme of the fifth-order Runge-Kutta Fehlberg method (Cash-Karp Runge-Kutta) for the above system of first-order equations is given as

$$f_{i+1} = f_i + h\left(\frac{2835}{27648}k_1 + \frac{18575}{48384}k_3 + \frac{13525}{55296}k_4 + \frac{277}{14336}k_5 + \frac{1}{4}k_6\right) \tag{40}$$

$$p_{i+1} = p_i + h\left(\frac{2835}{27648}l_1 + \frac{18575}{48384}l_3 + \frac{13525}{55296}l_4 + \frac{277}{14336}l_5 + \frac{1}{4}l_6\right) \tag{41}$$

$$q_{i+1} = q_i + h\left(\frac{2835}{27648}m_1 + \frac{18575}{48384}m_3 + \frac{13525}{55296}m_4 + \frac{277}{14336}m_5 + \frac{1}{4}m_6\right) \tag{42}$$

$$w_{i+1} = w_i + h\left(\frac{2835}{27648}n_1 + \frac{18575}{48384}n_3 + \frac{13525}{55296}n_4 + \frac{277}{14336}n_5 + \frac{1}{4}n_6\right) \tag{43}$$

$$z_{i+1} = z_i + h\left(\frac{2835}{27648}r_1 + \frac{18575}{48384}r_3 + \frac{13525}{55296}r_4 + \frac{277}{14336}r_5 + \frac{1}{4}r_6\right) \tag{44}$$

where

$$k_1 = a(\eta_i, f_i, p_i, q_i, w_i, z_i)$$

$$l_1 = b(\eta_i, f_i, p_i, q_i, w_i, z_i)$$

$$m_1 = c(\eta_i, f_i, p_i, q_i, w_i, z_i)$$

$$n_1 = d(\eta_i, f_i, p_i, q_i, w_i, z_i)$$

$$r_1 = e(\eta_i, f_i, p_i, q_i, w_i, z_i)$$

$$k_2 = a\left(\eta_i + \frac{1}{5}h,\ f_i + \frac{1}{5}k_1h,\ p_i + \frac{1}{5}l_1h,\ q_i + \frac{1}{5}m_1h,\ w_i + \frac{1}{5}n_1h,\ z_i + \frac{1}{5}r_1h\right)$$

$$l_2 = b\left(\eta_i + \frac{1}{5}h,\ f_i + \frac{1}{5}k_1h,\ p_i + \frac{1}{5}l_1h,\ q_i + \frac{1}{5}m_1h,\ w_i + \frac{1}{5}n_1h,\ z_i + \frac{1}{5}r_1h\right)$$

$$m_2 = c\left(\eta_i + \frac{1}{5}h,\ f_i + \frac{1}{5}k_1h,\ p_i + \frac{1}{5}l_1h,\ q_i + \frac{1}{5}m_1h,\ w_i + \frac{1}{5}n_1h,\ z_i + \frac{1}{5}r_1h\right)$$

$$n_2 = d\left(\eta_i + \frac{1}{5}h,\ f_i + \frac{1}{5}k_1h,\ p_i + \frac{1}{5}l_1h,\ q_i + \frac{1}{5}m_1h,\ w_i + \frac{1}{5}n_1h,\ z_i + \frac{1}{5}r_1h\right)$$

$$r_2 = e\left(\eta_i + \frac{1}{5}h,\ f_i + \frac{1}{5}k_1h,\ p_i + \frac{1}{5}l_1h,\ q_i + \frac{1}{5}m_1h,\ w_i + \frac{1}{5}n_1h,\ z_i + \frac{1}{5}r_1h\right)$$

$$k_3 = a\left(\begin{array}{l}\eta_i + \frac{3}{10}h,\ f_i + \frac{3}{40}k_1h + \frac{9}{40}k_2h,\ p_i + \frac{3}{40}l_1h + \frac{9}{40}l_2h,\\ q_i + \frac{3}{40}m_1h + \frac{9}{40}m_2h,\ w_i + \frac{3}{40}n_1h + \frac{9}{40}n_2h,\ z_i + \frac{3}{40}r_1h + \frac{9}{40}r_2h\end{array}\right)$$

$$l_3 = b\left(\begin{array}{l}\eta_i + \frac{3}{10}h,\ f_i + \frac{3}{40}k_1h + \frac{9}{40}k_2h,\ p_i + \frac{3}{40}l_1h + \frac{9}{40}l_2h,\\ q_i + \frac{3}{40}m_1h + \frac{9}{40}m_2h,\ w_i + \frac{3}{40}n_1h + \frac{9}{40}n_2h,\ z_i + \frac{3}{40}r_1h + \frac{9}{40}r_2h\end{array}\right)$$

$$m_3 = c\left(\begin{array}{l}\eta_i + \frac{3}{10}h,\ f_i + \frac{3}{40}k_1h + \frac{9}{40}k_2h,\ p_i + \frac{3}{40}l_1h + \frac{9}{40}l_2h,\\ q_i + \frac{3}{40}m_1h + \frac{9}{40}m_2h,\ w_i + \frac{3}{40}n_1h + \frac{9}{40}n_2h,\ z_i + \frac{3}{40}r_1h + \frac{9}{40}r_2h\end{array}\right)$$

$$n_3 = d\left(\begin{array}{l}\eta_i + \frac{3}{10}h,\ f_i + \frac{3}{40}k_1h + \frac{9}{40}k_2h,\ p_i + \frac{3}{40}l_1h + \frac{9}{40}l_2h,\\ q_i + \frac{3}{40}m_1h + \frac{9}{40}m_2h,\ w_i + \frac{3}{40}n_1h + \frac{9}{40}n_2h,\ z_i + \frac{3}{40}r_1h + \frac{9}{40}r_2h\end{array}\right)$$

$$r_3 = e\left(\begin{array}{l}\eta_i + \frac{3}{10}h,\ f_i + \frac{3}{40}k_1h + \frac{9}{40}k_2h,\ p_i + \frac{3}{40}l_1h + \frac{9}{40}l_2h,\\ q_i + \frac{3}{40}m_1h + \frac{9}{40}m_2h,\ w_i + \frac{3}{40}n_1h + \frac{9}{40}n_2h,\ z_i + \frac{3}{40}r_1h + \frac{9}{40}r_2h\end{array}\right)$$

$$k_4 = a\left(\begin{array}{l}\eta_i + \frac{3}{5}h,\ f_i + \frac{3}{10}k_1h - \frac{9}{10}k_2h + \frac{6}{5}k_3h,\ p_i + \frac{3}{10}l_1h - \frac{9}{10}l_2h + \frac{6}{5}l_3h,\\ q_i + \frac{3}{10}m_1h - \frac{9}{10}m_2h + \frac{6}{5}m_3h,\ w_i + \frac{3}{10}n_1h - \frac{9}{10}n_2h + \frac{6}{5}n_3h,\\ z_i + \frac{3}{10}r_1h - \frac{9}{10}r_2h + \frac{6}{5}r_3h\end{array}\right)$$

$$l_4 = b\left(\begin{array}{l}\eta_i + \frac{3}{5}h,\ f_i + \frac{3}{10}k_1h - \frac{9}{10}k_2h + \frac{6}{5}k_3h,\ p_i + \frac{3}{10}l_1h - \frac{9}{10}l_2h + \frac{6}{5}l_3h,\\ q_i + \frac{3}{10}m_1h - \frac{9}{10}m_2h + \frac{6}{5}m_3h,\ w_i + \frac{3}{10}n_1h - \frac{9}{10}n_2h + \frac{6}{5}n_3h,\\ z_i + \frac{3}{10}r_1h - \frac{9}{10}r_2h + \frac{6}{5}r_3h\end{array}\right)$$

$$m_4 = c\left(\begin{array}{l}\eta_i + \frac{3}{5}h,\ f_i + \frac{3}{10}k_1h - \frac{9}{10}k_2h + \frac{6}{5}k_3h,\ p_i + \frac{3}{10}l_1h - \frac{9}{10}l_2h + \frac{6}{5}l_3h,\\ q_i + \frac{3}{10}m_1h - \frac{9}{10}m_2h + \frac{6}{5}m_3h,\ w_i + \frac{3}{10}n_1h - \frac{9}{10}n_2h + \frac{6}{5}n_3h,\\ z_i + \frac{3}{10}r_1h - \frac{9}{10}r_2h + \frac{6}{5}r_3h\end{array}\right)$$

$$n_4 = d\left(\begin{array}{l}\eta_i + \frac{3}{5}h,\ f_i + \frac{3}{10}k_1h - \frac{9}{10}k_2h + \frac{6}{5}k_3h,\ p_i + \frac{3}{10}l_1h - \frac{9}{10}l_2h + \frac{6}{5}l_3h,\\ q_i + \frac{3}{10}m_1h - \frac{9}{10}m_2h + \frac{6}{5}m_3h,\ w_i + \frac{3}{10}n_1h - \frac{9}{10}n_2h + \frac{6}{5}n_3h,\\ z_i + \frac{3}{10}r_1h - \frac{9}{10}r_2h + \frac{6}{5}r_3h\end{array}\right)$$

$$r_4 = e\left(\begin{array}{l}\eta_i + \frac{3}{5}h,\ f_i + \frac{3}{10}k_1h - \frac{9}{10}k_2h + \frac{6}{5}k_3h,\ p_i + \frac{3}{10}l_1h - \frac{9}{10}l_2h + \frac{6}{5}l_3h,\\ q_i + \frac{3}{10}m_1h - \frac{9}{10}m_2h + \frac{6}{5}m_3h,\ w_i + \frac{3}{10}n_1h - \frac{9}{10}n_2h + \frac{6}{5}n_3h,\\ z_i + \frac{3}{10}r_1h - \frac{9}{10}r_2h + \frac{6}{5}r_3h\end{array}\right)$$

$$k_5 = a\left(\begin{array}{l}\eta_i + h,\ f_i - \frac{11}{54}k_1h + \frac{5}{2}k_2h - \frac{70}{27}k_3h + \frac{35}{27}k_4h,\ p_i - \frac{11}{54}l_1h + \frac{5}{2}l_2h - \frac{70}{27}l_3h + \frac{35}{27}l_4h,\\ q_i - \frac{11}{54}m_1h + \frac{5}{2}m_2h - \frac{70}{27}m_3h + \frac{35}{27}m_4h,\ w_i - \frac{11}{54}n_1h + \frac{5}{2}n_2h - \frac{70}{27}n_3h + \frac{35}{27}n_4h,\\ z_i - \frac{11}{54}r_1h + \frac{5}{2}r_2h - \frac{70}{27}r_3h + \frac{35}{27}r_4h\end{array}\right)$$

$$l_5 = b\left(\begin{array}{l}\eta_i + h,\ f_i - \frac{11}{54}k_1h + \frac{5}{2}k_2h - \frac{70}{27}k_3h + \frac{35}{27}k_4h,\ p_i - \frac{11}{54}l_1h + \frac{5}{2}l_2h - \frac{70}{27}l_3h + \frac{35}{27}l_4h,\\ q_i - \frac{11}{54}m_1h + \frac{5}{2}m_2h - \frac{70}{27}m_3h + \frac{35}{27}m_4h,\ w_i - \frac{11}{54}n_1h + \frac{5}{2}n_2h - \frac{70}{27}n_3h + \frac{35}{27}n_4h,\\ z_i - \frac{11}{54}r_1h + \frac{5}{2}r_2h - \frac{70}{27}r_3h + \frac{35}{27}r_4h\end{array}\right)$$

$$m_5 = c\left(\begin{array}{l}\eta_i + h,\ f_i - \frac{11}{54}k_1h + \frac{5}{2}k_2h - \frac{70}{27}k_3h + \frac{35}{27}k_4h,\ p_i - \frac{11}{54}l_1h + \frac{5}{2}l_2h - \frac{70}{27}l_3h + \frac{35}{27}l_4h,\\ q_i - \frac{11}{54}m_1h + \frac{5}{2}m_2h - \frac{70}{27}m_3h + \frac{35}{27}m_4h,\ w_i - \frac{11}{54}n_1h + \frac{5}{2}n_2h - \frac{70}{27}n_3h + \frac{35}{27}n_4h,\\ z_i - \frac{11}{54}r_1h + \frac{5}{2}r_2h - \frac{70}{27}r_3h + \frac{35}{27}r_4h\end{array}\right)$$

$$n_5 = c\left(\begin{array}{l}\eta_i + h,\ f_i - \frac{11}{54}k_1h + \frac{5}{2}k_2h - \frac{70}{27}k_3h + \frac{35}{27}k_4h,\ p_i - \frac{11}{54}l_1h + \frac{5}{2}l_2h - \frac{70}{27}l_3h + \frac{35}{27}l_4h,\\ q_i - \frac{11}{54}m_1h + \frac{5}{2}m_2h - \frac{70}{27}m_3h + \frac{35}{27}m_4h,\ w_i - \frac{11}{54}n_1h + \frac{5}{2}n_2h - \frac{70}{27}n_3h + \frac{35}{27}n_4h,\\ z_i - \frac{11}{54}r_1h + \frac{5}{2}r_2h - \frac{70}{27}r_3h + \frac{35}{27}r_4h\end{array}\right)$$

$$r_5 = d\left(\begin{array}{l}\eta_i + h,\ f_i - \frac{11}{54}k_1h + \frac{5}{2}k_2h - \frac{70}{27}k_3h + \frac{35}{27}k_4h,\ p_i - \frac{11}{54}l_1h + \frac{5}{2}l_2h - \frac{70}{27}l_3h + \frac{35}{27}l_4h,\\ q_i - \frac{11}{54}m_1h + \frac{5}{2}m_2h - \frac{70}{27}m_3h + \frac{35}{27}m_4h,\ w_i - \frac{11}{54}n_1h + \frac{5}{2}n_2h - \frac{70}{27}n_3h + \frac{35}{27}n_4h,\\ z_i - \frac{11}{54}r_1h + \frac{5}{2}r_2h - \frac{70}{27}r_3h + \frac{35}{27}r_4h\end{array}\right)$$

$$k_6 = a\left(\begin{array}{l}\eta_i + \frac{7}{8}h,\ f_i + \frac{1631}{55296}k_1h + \frac{175}{512}k_2h + \frac{575}{13824}k_3h + \frac{44275}{110592}k_4h + \frac{253}{4096}k_5h,\\ p_i + \frac{1631}{55296}l_1h + \frac{175}{512}l_2h + \frac{575}{13824}l_3h + \frac{44275}{110592}l_4h + \frac{253}{4096}l_5h,\\ q_i + \frac{1631}{55296}m_1h + \frac{175}{512}m_2h + \frac{575}{13824}m_3h + \frac{44275}{110592}m_4h + \frac{253}{4096}m_5h,\\ n_i + \frac{1631}{55296}w_1h + \frac{175}{512}w_2h + \frac{575}{13824}w_3h + \frac{44275}{110592}w_4h + \frac{253}{4096}w_5h,\\ z_i + \frac{1631}{55296}r_1h + \frac{175}{512}r_2h + \frac{575}{13824}r_3h + \frac{44275}{110592}r_4h + \frac{253}{4096}r_5h\end{array}\right)$$

$$l_6 = b\left(\begin{array}{l}\eta_i + \frac{7}{8}h,\ f_i + \frac{1631}{55296}k_1h + \frac{175}{512}k_2h + \frac{575}{13824}k_3h + \frac{44275}{110592}k_4h + \frac{253}{4096}k_5h,\\ p_i + \frac{1631}{55296}l_1h + \frac{175}{512}l_2h + \frac{575}{13824}l_3h + \frac{44275}{110592}l_4h + \frac{253}{4096}l_5h,\\ q_i + \frac{1631}{55296}m_1h + \frac{175}{512}m_2h + \frac{575}{13824}m_3h + \frac{44275}{110592}m_4h + \frac{253}{4096}m_5h,\\ n_i + \frac{1631}{55296}w_1h + \frac{175}{512}w_2h + \frac{575}{13824}w_3h + \frac{44275}{110592}w_4h + \frac{253}{4096}w_5h,\\ z_i + \frac{1631}{55296}r_1h + \frac{175}{512}r_2h + \frac{575}{13824}r_3h + \frac{44275}{110592}r_4h + \frac{253}{4096}r_5h\end{array}\right)$$

$$m_6 = c\begin{pmatrix} \eta_i + \frac{7}{8}h,\ f_i + \frac{1631}{55296}k_1h + \frac{175}{512}k_2h + \frac{575}{13824}k_3h + \frac{44275}{110592}k_4h + \frac{253}{4096}k_5h, \\ p_i + \frac{1631}{55296}l_1h + \frac{175}{512}l_2h + \frac{575}{13824}l_3h + \frac{44275}{110592}l_4h + \frac{253}{4096}l_5h, \\ q_i + \frac{1631}{55296}m_1h + \frac{175}{512}m_2h + \frac{575}{13824}m_3h + \frac{44275}{110592}m_4h + \frac{253}{4096}m_5h, \\ n_i + \frac{1631}{55296}w_1h + \frac{175}{512}w_2h + \frac{575}{13824}w_3h + \frac{44275}{110592}w_4h + \frac{253}{4096}w_5h, \\ z_i + \frac{1631}{55296}r_1h + \frac{175}{512}r_2h + \frac{575}{13824}r_3h + \frac{44275}{110592}r_4h + \frac{253}{4096}r_5h \end{pmatrix}$$

$$n_6 = d\begin{pmatrix} \eta_i + \frac{7}{8}h,\ f_i + \frac{1631}{55296}k_1h + \frac{175}{512}k_2h + \frac{575}{13824}k_3h + \frac{44275}{110592}k_4h + \frac{253}{4096}k_5h, \\ p_i + \frac{1631}{55296}l_1h + \frac{175}{512}l_2h + \frac{575}{13824}l_3h + \frac{44275}{110592}l_4h + \frac{253}{4096}l_5h, \\ q_i + \frac{1631}{55296}m_1h + \frac{175}{512}m_2h + \frac{575}{13824}m_3h + \frac{44275}{110592}m_4h + \frac{253}{4096}m_5h, \\ n_i + \frac{1631}{55296}w_1h + \frac{175}{512}w_2h + \frac{575}{13824}w_3h + \frac{44275}{110592}w_4h + \frac{253}{4096}w_5h, \\ z_i + \frac{1631}{55296}r_1h + \frac{175}{512}r_2h + \frac{575}{13824}r_3h + \frac{44275}{110592}r_4h + \frac{253}{4096}r_5h \end{pmatrix}$$

$$r_6 = e\begin{pmatrix} \eta_i + \frac{7}{8}h,\ f_i + \frac{1631}{55296}k_1h + \frac{175}{512}k_2h + \frac{575}{13824}k_3h + \frac{44275}{110592}k_4h + \frac{253}{4096}k_5h, \\ p_i + \frac{1631}{55296}l_1h + \frac{175}{512}l_2h + \frac{575}{13824}l_3h + \frac{44275}{110592}l_4h + \frac{253}{4096}l_5h, \\ q_i + \frac{1631}{55296}m_1h + \frac{175}{512}m_2h + \frac{575}{13824}m_3h + \frac{44275}{110592}m_4h + \frac{253}{4096}m_5h, \\ n_i + \frac{1631}{55296}w_1h + \frac{175}{512}w_2h + \frac{575}{13824}w_3h + \frac{44275}{110592}w_4h + \frac{253}{4096}w_5h, \\ z_i + \frac{1631}{55296}r_1h + \frac{175}{512}r_2h + \frac{575}{13824}r_3h + \frac{44275}{110592}r_4h + \frac{253}{4096}r_5h \end{pmatrix}$$

Using theabove fifth-order Runge-Kutta Fehlberg method coupled with shooting method,computer programs are written in MATLAB for the solutions of the Eq. (14). The results for step size, $h = 0.01$ are presented in the following section.

Results and Discussion

The results of the solutions of the nonlinear model with the aid of homotopy analysis method (HAM) is compared with the results of the fifth-order Runge-Kutta Fehlberg method (RKFNM) coupled with shooting method as shown in in (Table 4). As observed from the Table, good agreement is established between the results of the numerical and homotopy analysis methods.

Table 4 Comparison of results of numerical and homotopy analysis method for *f(η)*, when $De = 0.1, Da^{-1} = \phi = M = 0, K = 0.1, Re_w = 4$

η	Rkfnm	ham	|rkfnm-ham|
0	0	0	0
0.05	0.070154	0.0701	2.89E-07
0.1	0.139997	0.139998	5.69E-07
0.15	0.209217	0.209218	8.33E-07
0.2	0.259219	0.259218	1.08E-06
0.25	0.344546	0.344548	1.29E-06
0.3	0.410038	0.41004	1.47E-06

Table continue

η	Rkfnm	ham	|rkfnm-ham|
0.35	0.473672	0.473674	1.61E-06
0.4	0.535148	0.535146	1.71E-06
0.45	0.594153	0.594155	1.75E-06
0.5	0.650402	0.650404	1.75E-06
0.55	0.7036	0.703599	1.7E-06
0.6	0.75345	0.753452	1.61E-06
0.65	0.79968	0.799682	1.47E-06
0.7	0.842013	0.842014	1.29E-06
0.75	0.880181	0.880182	1.08E-06
0.8	0.913929	0.913929	8.45E-07
0.85	0.94301	0.943011	6.05E-07

Using copper nanoparticle and water, the results obtained from the analytical solutionare shown graphically in Figs. 2-9, when $Re_w = 8, De = 0.1, M = 2, \hbar = 0.1, D_a = 2$ and $\phi = 0.01$, unless otherwise stated. Figure. illustrate the influence of nano particle concentration (ϕ) on the flow process. As shown from the Figure, the quantitative increase of the nano particle concentration causes increase in the velocity distribution. It is very important to indicate viscoelastic nature of the fluid. Therefore, the effects of Deborah's number on the flow process are depicted in Fig. 3. It illustrated in that increase in Deborah's number (De) which illustrates the UCM as highly elastic fluid (such as polymeric melts) depicts decrease in fluid flow velocity.

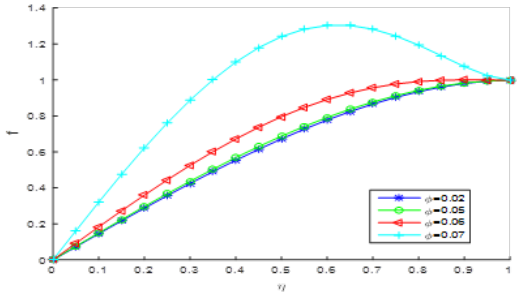

Figure 2 Effect of nanoparticle concentration number (ϕ) on the axial velocity of the flow process.

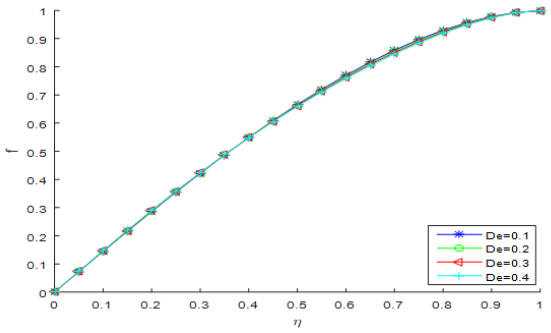

Figure 3 Effect of Deborah's number (De) onthe axial velocity of the flow process.

The influence of magnetic field parameter on flow of the UCM fluid under is depicted in (Figure 4). As observed in the figure, the numerical increase of the magnetic or Hartmann parameter (M) shows decreasing velocity profile. This is because the applied magnetic field produces a damping effect (Lorentz force) on the flow process. This damping effects increases as the quantitative or numerical value of the Hartmann number increases. It should be noted that the effects magnetic field parameter is maximum towards the upper flow channel. In order to shown the effect of the permeability of the porous medium on the flow, effect of Darcy parameter (Da) on fluid transport is illustrated in (Figure 5) Increasing Darcy number demonstrates increasing velocity profile as shown in the figure.

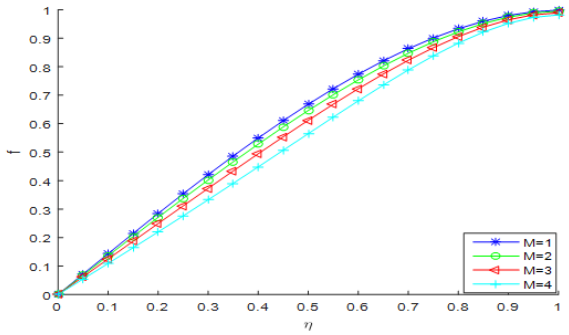

Figure 4 Effect of Hartmann parameter (M) on the axial velocity of the flow process.

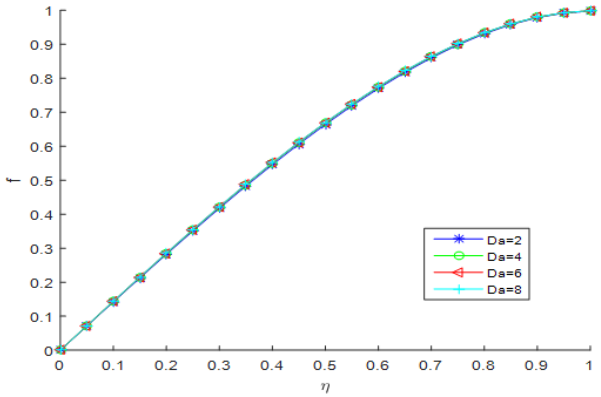

Figure 5 Effect of Darcy's number (Da) onthe axial velocity of the flow process.

(Figure 6) shows the effect of fluid slip parameter (k) on the velocity of the fluid flow. It should be noted that the slip parameter depicts that the fluid velocity at the boundary is not at equal velocity with fluid particles closest to flow boundary due to large variance in macro and micro fluid flow. As observed from the (Figure 6) increasing the slip parameter leads to decreasing velocity distributions of the process. In order to show the relative significance of the inertia effect as compared to the viscous effect, the effect of Reynolds number on the flow phenomena is illustrated in the (Figure 7). It is established form the graphical display that increasing Reynolds number (Re_w) causes decrease in flow profile which effect is maximum towards the upper plate.

It is shown that increasing the Reynolds number causes decrease in velocity distribution but as flow reaches the mid plate around $\eta = 0.5$ (not determined accurately) an increasing velocity distribution is seen. However, effect is minimal towards the upper plate. Also, influence of magnetic field on radial velocity is depicted in (Figure 9). as shown significant increase in velocity is seen due to quantitative increase of Hartmann parameter (M) towards the lower plate while as upper plate is approached a reverse trend is observed.

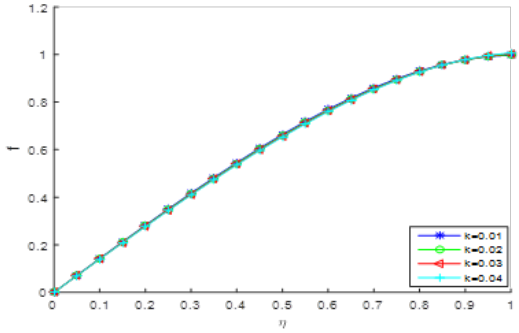

Figure 6 Effect of slip parameter (k) on the axial velocity of the flow process.

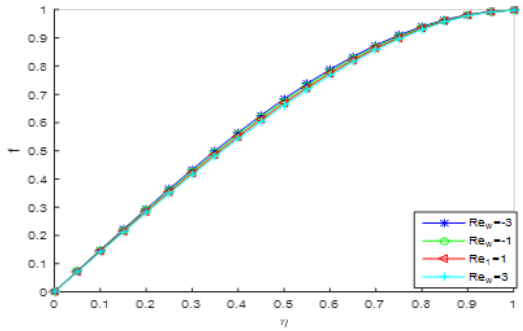

Figure 7 Effect of Reynold's number (Re_w) onthe axial velocity of the flow process.

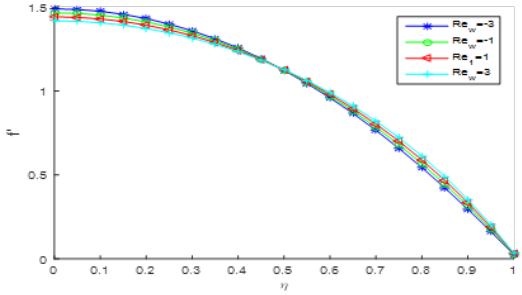

Figure 8 Effect of Reynold's number (Re_w) onthe radial velocity of the flow process.

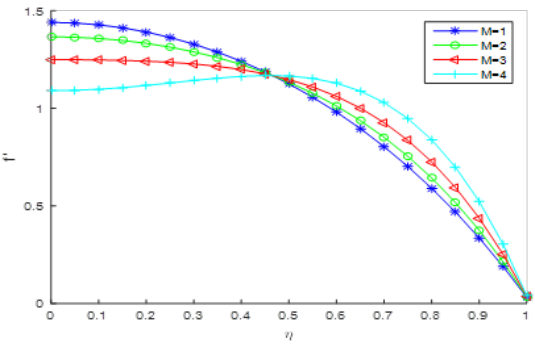

Figure 9 Effect of Hartman parameter (M) on the radial velocity of the flow process.

Citation: Sobamowo MG, Yinusa AA, Akinshilo AT, et al. Homotopy analysis method to MHD-slip flow of an upper- convected maxwell viscoelastic nanofluid in a permeable channel embedded in a porous medium. *Int J Petrochem Sci Eng.* 2020;5(1):11–20. DOI: 10.15406/ipcse.2020.05.00118

Conclusion

In this work, analysis of upper convective Maxwell (UCM) nano fluid flow through a permeable microchannel embedded in a porous medium and under the influence of slip condition has been presented. Important fluid parameter effect such as Deborah's number, Darcy parameter and Hartman parameter were investigated on flow. that increase in slip parameter, nano particle concentration and Darcy number lead to increase in the velocity of the upper-convected Maxwell fluid while increase in Deborah's, Hartmann, and Reynolds numbers decrease the fluid flow velocity towards the lower plate but as the upper plate is approached a reverse trend is observed. The results obtained in this work may be used to further UCM fluid in applications in biomedical, astrophysics, geosciences etc.

Data availability Statement

The data used in this work can be found in open documents in public domain.

Acknowledgments

The authors express sincere appreciation to University of Lagos, Nigeria for providing material supports and good environment for this work.

Funding statement

This research was performed as part of the employment of the authors under the University of Lagos, Nigeria.

Conflicts of interest

The authors declare that there is no conflict of interest regarding the publication of this paper.

References

1. R B Bird, R C. Armstrong O. Dynamics of polymeric liquids,vols I and II. *Wiley New York.* 1987.
2. K Sadeghy, AH Najafi, M Saffaripour. Sakiadis flow of an upper-convected maxwell fluid. *International Journal of Non-Linear Mechanics.* 2005;40:1220–1228.
3. Z Ziabaksh G Domairry. Solution of laminar viscous flow in semi porous channel in the presence of a uniform magnetic field by using homotopy analysis method. *Communications in nonlinear science and numerical simulations*. 2009;14(4):1284–1294.
4. C Fetecau. A new exact solution for the flow of a maxwell fluid past an infinite plate. *International Journal of Non-Linear Mechanics* . 2003;38:423–427.
5. JCR Hunt. Magnetohydrodynamic flow in rectangular ducts. *Journal of Fluid Mechanics*. 1965;21:577–590.
6. M Sheikholeslami, M Hatami, DD Ganji. Analytical investigation of MHD nanofluid flow in a semi-porous channel. *Powder Technology.* 2013;246:327–336.
7. M Sheikholeslami, MGorji-Bandpy DD. Ganji. numerical investigation of MHD effects on Al2O3-water nanofluid flow and heat transfer in a semi-annulus using LBM Energy. 2013; 60:501–510.
8. M Sheikholeslami, M Gorji-Bandpy, DD Gnaji. Lattice boltzman method for MHD natural convection heat transfer using nano fluid. *Powder Technology.* 2014;254:82–93.
9. M Sheikholeslami, MHatami, DD Ganji. Nano fluid flow and heat transfer in a rotating system in the presence of a magnetic field. *Journal of Molecular Liquid*. 2014;190:112–120.
10. B Raftari ,A Yildirim. The application of homotopy perturbation method for MHD flows above porous stretching sheets. *Computational Applied Mechanics.* 2010;59:740–744.
11. M Sheikholeslami, DD Ganji. Entropy generation of nanofluid in presence of magnetic field using lattice boltzmann method. *Physica A.* 2015;417:273–286.
12. DD Ganji, H Kachapi, H Seyed. Analytical and numerical method in engineering and applied science. *Progress Nonlinear Science.* 2011;3:570–579.
13. K Sadeghy M Sharifi. Local similarity solution for the flow of a "second grade" viscoelastic fluid above a moving plate. *International Journal of Non-Linear Mechanics.* 2004;39:1265-1273.
14. K Vajrevulu, K V Prasad, A Sujatha. MHD flow and mass transfer of chemically reactive upper convected maxwell fluid past porous surface. *Applied Mathematical Mechanics.* 2012;33(7): 899-910.
15. B Raftari KVajrevulu. Homotopy analysis method for MHD viscoelastic fluid flow and heat transfer in a channel with a stretching wall. *Communications Nonlinear Science Simulation*. 2012;17(11):4149–4162.
16. M Hatami, R Nouri ,DD Ganji. Forced convection analysis for MHD Al_2O_3-water nanofluid flow over a horizontal plate. *Journal of Molecular Liquid.* 2013;187:294–301.
17. Aziz. A similarity solution for laminar thermal boundary layer over a flat plat with a convective surface boundary condition. *Communication Nonlinear Science Numerical Simulation.* 2009;14:1064–1068.
18. OA Beg, OD Makinde. Viscoelastic flow and species transfer in a darcian high permeability channel. *Journal of Petrol Science Engineering* 2011;76: 93–99.
19. CLMH. Navier. Memoir sur les lois du movement des fluids. *Memoirs Academic Royal Science Institute France*.1823;6:389-440.
20. CH Choi, JA Westin, KS Breur. To slip or not slip water flows in hydrophilic and hydrophobic microchannels. *Proceedings of IMECE New Orleans LA Article ID.* 2002;33:707.
21. M T Matthew, ID Boyd. Nano boundary layer equation with nonlinear Navier boundary condition. *Journal of Mathematical Analysis and Application*. 2007;333:381–400.
22. M J Martin LD Boyd. Momentum and heat transfer in a laminar boundary layer with slip flow. *Journal of Thermo physics and Heat Transfer.* 2006; 20(4):710–719.
23. P D Ariel. Axisymmetric flow due to stretching sheet with partial slip. *Computer and Mathematics with Application*. 2007;333:381–400.
24. C Wang. Analysis of viscous flow due to a stretching sheet with surface slip and suction. *Nonlinear Analysis: Real world application.* 2009;10(1) :375–380.
25. K Das. Impact of thermal radiation on MHD slip flow over a flat plate with variable fluid properties. *Heat and mass transfer*. 2012;48:767–778.
26. K Das. Slip effects on heat and mass transfer in MHD micro polar fluid flow over an inclined plate with thermal radiation and chemical reaction. *International Journal of Numerical methods in Fluids*. 2016;70:96-101.
27. Hussain ST. Mohyud-Cheema, TA Din. Analytical and numerical approaches to squeezing flow and heat transfer between two parallel disks with velocity slip and temperature jump. *China Physics Letter*. 2012;29:1-5.

28. K Das. Slip flow and convective heat transfer of nanofluid over a permeable stretching surface. *Computers and Physics.*2012;64(1):34-42.

29. RG Deissler. An analysis of second-order slip flow and temperature-jump boundary conditions for rarefied gases*. International Journal of heat and mass transfer*. 1964;7(6):681-694.

30. K Das, Jana S, Acharya N. Slip effects on squeezing flow of nanofluid between two parallel disks. *International Journal of Applied Mechanics and Engineering*. 2016;21(1):5-20.

31. R Ellahi, Hayat T, Mahomed FM. Effects of slip on nonlinear flows of a third grade fluid*. NonlinearAnalysis: Real world Applications.* 2010;11:139-146.

32. Malvadi, F Hedayati, DD Ganji. Slip effects on unsteady stagnation pointflow of a nanofluid over a stretching sheet. *Powder Technology*. 2014;253:377-384.

33. M Abbasi, M Khaki, A Rahbari, DD. Ganji. Analysis of MHD flow characteristics of an UCM viscoelastic flow in a permeable channel under slip conditions. *Journal of Brazilian Society of Mechanical Engineering Science*. 2015:25-5.

34. SJ Liao. The proposed homotopy analysis technique for the solution of nonlinear problems. *PhD thesis Shanghai Jiao Tong University*.1992.

35. SJ Liao. Beyond perturbation: Introduction to the homotopy analysis method. *Chapman Hall CRC Press Boca Raton.* 2003.

36. SJ Liao. On the homotopy analysis method for nonlinear problems. *Applied Mathematical Computation.* 2004;47 (2):499-513.

37. S J Liao. An approximate solution technique not depending on small parameters: a special example. *International Journal of Non-Linear Mechanics.*1995;303:371-380.